

# GNSS Ambiguity Resolution by Adaptive Mixture Kalman Filter

Berntorp, K.; Weiss, A.; Di Cairano, S.

TR2018-103 July 13, 2018

## Abstract

The precision of global navigation satellite systems (GNSSs) relies heavily on accurate carrier phase ambiguity resolution. The ambiguities are known to take integer values, but the set of ambiguity values is unbounded. We propose a mixture Kalman filter solution to GNSS ambiguity resolution. By marginalizing out the set of ambiguities and exploiting a likelihood proposal for generating the ambiguities, we can bound the possible values to a tight and dense set of integers, which allows for extracting the integer solution as a maximum likelihood estimate from a mixture Kalman filter. We verify the efficacy of the approach in simulation including a comparison with a well-known integer least-squares based method. The results indicate that our proposed switched mixture Kalman filter repeatedly finds the correct integers in cases where the other method fails.

*International Conference on Information Fusion (FUSION)*

This work may not be copied or reproduced in whole or in part for any commercial purpose. Permission to copy in whole or in part without payment of fee is granted for nonprofit educational and research purposes provided that all such whole or partial copies include the following: a notice that such copying is by permission of Mitsubishi Electric Research Laboratories, Inc.; an acknowledgement of the authors and individual contributions to the work; and all applicable portions of the copyright notice. Copying, reproduction, or republishing for any other purpose shall require a license with payment of fee to Mitsubishi Electric Research Laboratories, Inc. All rights reserved.



# GNSS Ambiguity Resolution by Adaptive Mixture Kalman Filter

Karl Berntorp<sup>1</sup>, Avishai Weiss<sup>1</sup>, and Stefano Di Cairano<sup>1</sup>

**Abstract**—The precision of global navigation satellite systems (GNSSs) relies heavily on accurate carrier phase ambiguity resolution. The ambiguities are known to take integer values, but the set of ambiguity values is unbounded. We propose a mixture Kalman filter solution to GNSS ambiguity resolution. By marginalizing out the set of ambiguities and exploiting a likelihood proposal for generating the ambiguities, we can bound the possible values to a tight and dense set of integers, which allows for extracting the integer solution as a maximum-likelihood estimate from a mixture Kalman filter. We verify the efficacy of the approach in simulation including a comparison with a well-known integer least-squares based method. The results indicate that our proposed switched mixture Kalman filter repeatedly finds the correct integers in cases where the other method fails.

## I. INTRODUCTION

Global navigation satellite systems (GNSS), such as GPS, Galileo, and QZSS, are used in many positioning and navigation applications world-wide, and GNSS receivers can be found, for example, in airplanes, cars, and cell phones. Generally, a GNSS receiver determines its position by triangulation using two types of measurements from several satellites orbiting the earth: pseudorange measurements and carrier phase measurements. The pseudorange measurement (or code measurement) is the range or distance between a GNSS receiver and each of a set of satellites and is determined by multiplying the signal travel time (from the satellite to the receiver) by the speed of light. Pseudoranges are inexact because they include errors due to, for instance, satellite clock timing error, ionospheric and tropospheric refraction effects, receiver tracking noise, and multipath error. To eliminate or reduce these errors, differential corrections are used in many GNSS applications [1]. The carrier phase measurement is obtained by integrating a reconstructed carrier of the signal as it arrives at the receiver. The carrier signal observations are more precise than the pseudorange measurements, and can be tracked with millimeter precision [2] within a wavelength. However, because of an unknown number of carrier cycles in transit between the satellite and the receiver when the receiver starts tracking the carrier phase of the signal, there is an integer ambiguity in the carrier phase measurement. Hence, correct integer ambiguity resolution is pivotal for high-precision GNSS.

An overview of traditional approaches for ambiguity resolution can be found in [3], and a summary of integer estimation theory is presented in [4]. Many GNSS ambiguity

resolution methods are based on two-stage approaches. First an estimation of a float-valued ambiguity, which forms the basis for a search for the integer value based on the float estimates. Subsequently, the two methods are often independent on each other. The method in [5] uses a Kalman filter approach to estimate the float ambiguity together with the state, whereas other methods use least squares [4]. The least-squares ambiguity decorrelation method (LAMBDA) [6]–[8] solves an integer least squares (ILS) problem in a two-stage procedure, starting from the real-valued least-squares solution (e.g., obtained from the Kalman filter). The first step comprises modifying the original ILS problem by decorrelating the ambiguities, and then searching for the optimal integers over a hyper-ellipsoidal region. The LAMBDA method has been further developed into the modified LAMBDA (MLAMBDA) [9], and related approaches can be found in [10], [11].

In this paper, we formulate the GNSS ambiguity resolution problem in a Bayesian framework as a joint GNSS receiver state and ambiguity parameter estimation problem. By exploiting marginalization, we can solve for the GNSS receiver state using a mixture Kalman filter, where each Kalman filter is conditioned on a particular possible fixed ambiguity for each satellite. The approach employs the marginalized particle filter [12] to determine the possible ambiguities.

Bayesian approaches have been considered before in the context of GNSS ambiguity resolution, see for example [13], which presents a solution similar to the case of fixed multiple models, and [14], which uses Bayesian statistics to derive confidence regions for a GPS application. An overview of multiple-model methods for GNSS ambiguity resolution can be found in [15]. For instance, [16] uses fixed multiple-model Kalman filters, where the ambiguities are the integers the models depend on. A similar approach is found in [17], where each of the filters uses a different set of ambiguities, and switched multiple-model estimators for detection of cycle slip (sudden loss of lock-up of the carrier signal) are found in [18]. A difficulty with multiple-model approaches is that the ambiguities can take any integer value, and straightforward application of a multiple-model approach is therefore computationally intractable. In [15], a procedure using the LAMBDA method to search for the integers to use in the different models is mentioned, starting from the float solution. However, this procedure then needs to be restarted as soon as a cycle slip or loss of contact with the satellite occurs (e.g., in urban areas).

Our approach differs from previous work in that we formulate the estimation problem in a particle-filtering context, where we marginalize out the ambiguities. Particle filters have

<sup>1</sup>The authors are with Mitsubishi Electric Research Laboratories (MERL), 02139 Cambridge, MA, USA. Email:karl.o.berntorp@ieee.org

been considered in relation to GNSS ambiguity resolution before. An early work is [19], which, however, does not consider the GNSS receiver state. The work in [20] uses particle filtering for combined inertial measurement aided GPS positioning, and [21], [22] both apply particle filtering for estimating the joint GNSS receiver state and ambiguities. However, estimating the joint state and ambiguities in a particle filter leads to an unnecessarily high-dimensional estimation problem, which is problematic in a real-time application because of the curse of dimensionality. Any motion model of the ambiguities is highly uncertain due to the unboundedness of the ambiguity set and lack of knowledge of how and when the ambiguities change. In our approach, by leveraging the optimal proposal density for the ambiguities, which for the uncertain ambiguity model corresponds to likelihood sampling, we can statistically bound the possible range of ambiguities and execute a mixture Kalman filter. The number of Kalman filters is made adaptive on the possible range of ambiguities. Hence, as the estimator narrows the ambiguity set, the number of particles decrease. In a simulation study, we show that our method correctly finds the integer ambiguities and can automatically detect cycle slip. Furthermore, a comparison study indicates that our method finds the correct integers in cases where other methods fail, and that the computational times are on the same order as previous approaches.

## II. PROBLEM SETUP

The pseudorange code and carrier phase measurements of a satellite measure the distance between the satellite and the target receiver. In our setup, we consider the pseudorange code and carrier phase measurements from the  $j$ th satellite to the receiver  $r$  at each time  $t_k$  at step (epoch)  $k$  modeled as [1], [4], [19], [21], [23],

$$P_k^j = \rho_k^j + c(\delta T_k - \delta t_k^j) + I_k^j \\ T_k^j + \epsilon_k^j, \quad (1a)$$

$$\Phi_k^j = \rho_k^j + c(\delta t_k - \delta t_k^j) - I_k^j \\ T_k^j + \lambda n^j + \eta_k^j, \quad (1b)$$

with notation as in Table I. The distance between the receiver and the  $j$ th satellite is defined as

$$\rho^j = \sqrt{(p_X^j - p_{X,r})^2 + (p_Y^j - p_{Y,r})^2 + (p_Z^j - p_{Z,r})^2}, \quad (2)$$

where  $\mathbf{p}^j = [p_X^j \ p_Y^j \ p_Z^j]^T$  and  $\mathbf{p}_r = [p_{X,r} \ p_{Y,r} \ p_{Z,r}]^T$  are the coordinates of the  $j$ th satellite and the receiver  $r$ , respectively, in the world-aligned coordinate frame. By utilizing a base receiver  $b$  mounted at a known location broadcasting to the original receiver  $r$  most of the sources of error can be removed, at least approximately. If we consider the observation equation (1) for the two receivers and form the difference between them (*single differencing*), the error due to the satellite clock bias can be eliminated. Furthermore, *double differentiation*, that is, the single difference between receivers differenced again between two satellites, can be used to eliminate, or suppress,

the other sources of error [21], [23]. The receiver clock error terms also vanish due to the single and double differentiation.

Let the single-differenced observation equations (1a) and (1b) between the receivers  $b$  and  $r$  observing satellite  $j$  at time step  $k$  be denoted with  $\Delta P_{br,k}^j = P_{b,k}^j - P_{r,k}^j$  and  $\Delta \Phi_{br,k}^j = \Phi_{b,k}^j - \Phi_{r,k}^j$ , respectively. We introduce the double-difference operator  $\nabla \Delta (\cdot)_{br,k}^{jl}$  for the double difference of two satellites  $j$  and  $l$ , which yields

$$\nabla \Delta P_{br,k}^{jl} = \Delta P_{br,k}^j - \Delta P_{br,k}^l \\ = \nabla \Delta \rho_{br,k}^{jl} + \nabla \Delta I_{br,k}^{jl} + \nabla \Delta \epsilon_{br,k}^{jl}, \quad (3a)$$

$$\nabla \Delta \Phi_{br,k}^{jl} = \Delta \Phi_{br,k}^j - \Delta \Phi_{br,k}^l \\ = \nabla \Delta \rho_{br,k}^{jl} - \nabla \Delta I_{br,k}^{jl} + \lambda \nabla \Delta n_{br}^{jl} + \nabla \Delta \eta_{br,k}^{jl}. \quad (3b)$$

Furthermore, for short distances between the two receivers (e.g., 30 km), ionospheric errors are small under double differencing, leading to

$$\nabla \Delta P_{br,k}^{jl} \approx \nabla \Delta \rho_{br,k}^{jl} + \nabla \Delta \epsilon_{br,k}^{jl}, \quad (4a)$$

$$\nabla \Delta \Phi_{br,k}^{jl} \approx \nabla \Delta \rho_{br,k}^{jl} + \lambda \nabla \Delta n_{br}^{jl} + \nabla \Delta \eta_{br,k}^{jl}. \quad (4b)$$

Subsequently, we will use observation equation (4) and leave (3) and other extensions, such as multipath effects, to future work. Furthermore, for notational convenience we will drop the use of  $\nabla \Delta$  and write

$$P_{br,k}^{jl} = \rho_{br,k}^{jl} + \epsilon_{br,k}^{jl}, \quad (5a)$$

$$\Phi_{br,k}^{jl} = \rho_{br,k}^{jl} + \lambda n_{br,k}^{jl} + \eta_{br,k}^{jl}, \quad (5b)$$

where  $\rho_{br,k}^{jl} = (\rho_{r,k}^j - \rho_{b,k}^j) - (\rho_{r,k}^l - \rho_{b,k}^l)$  and similar for the other quantities. We assume that the measurement noise  $\epsilon_{br}^{jl}$  and  $\eta_{br}^{jl}$  are zero-mean Gaussian distributed with known covariance  $\sigma_\epsilon$ ,  $\sigma_\eta$  (where  $\sigma_\epsilon \gg \sigma_\eta$  [1], [21]), that is,

$$\begin{bmatrix} \epsilon_{br,k}^{jl} \\ \eta_{br,k}^{jl} \end{bmatrix} \sim \mathcal{N} \left( \mathbf{0}, \begin{bmatrix} \sigma_\epsilon & 0 \\ 0 & \sigma_\eta \end{bmatrix} \right). \quad (6)$$

We assume that there are  $M - 1$  double-differenced observations (5), that is, the measurement vector  $\mathbf{y} \in \mathbb{R}^{2(M-1)}$  and the vector of integer ambiguities  $\mathbf{n} \in \mathbb{Z}^{M-1}$ .

The objective in this paper is to resolve the unknown receiver position  $\mathbf{p}_{r,k}$  at each time step  $k$  and the set of unknown integer ambiguities  $\mathbf{n}$  from the measurements  $\mathbf{y}_{0:k} = \{\mathbf{y}_0, \dots, \mathbf{y}_k\}$ . While the integer ambiguities are typically constant for extended periods of time, they may change abruptly as soon as a loss-of-lock of tracking of the satellite occurs, for instance, due to shadowing effects in urban areas or cycle slip.

## III. GNSS INTEGER AMBIGUITY AND POSITION RESOLUTION

This section presents the proposed method for joint positioning and integer ambiguity resolution. We approach the problem in a fully Bayesian context and rely on a mixture Kalman filter approach with adaptation of the number of Kalman filters to the uncertainty in the ambiguity estimates.

TABLE I  
NOTATION FOR THE CODE AND PSEUDORANGE MEASUREMENT EQUATIONS.

Notation	Description	Unit
$P$	Code observation	m
$\rho$	Distance between the receiver and the satellite	m
$c$	Speed of light	m/s
$\delta T$	Receiver clock bias	s
$\delta t$	Satellite clock bias	s
$I$	Ionospheric delay	m
$T$	Tropospheric delay	m
$\epsilon$	Code observation noise	m
$\lambda$	Carrier wavelength	m
$\Phi$	Carrier phase observation	m
$n$	Integer ambiguity	cycles
$\eta$	Carrier observation noise	m

### A. Estimation Model

We consider the case of kinematic positioning in short baseline conditions, where ionospheric delays can be ignored. Without loss of generality, the first satellite is assumed to be the reference satellite, that is,  $j = 1$ . We form the observation equations at each time step  $k$  based on the double-differenced measurements (5),

$$\mathbf{y}_k = [P_{br,k}^{12} \dots P_{br,k}^{1M} \Phi_{br,k}^{12} \dots \Phi_{br,k}^{1M}]^T, \quad (7)$$

and the corresponding measurement model is

$$\mathbf{y}_k = \mathbf{h}_k + \lambda \bar{\mathbf{n}}_k + \mathbf{e}_k, \quad (8)$$

where

$$\mathbf{h}_k = [\rho_{br,k}^{12} \dots \rho_{br,k}^{1M} \rho_{br,k}^{12} \dots \rho_{br,k}^{1M}]^T, \quad (9a)$$

$$\bar{\mathbf{n}}_k = [0 \dots 0 \mathbf{n}_k^T]^T, \quad (9b)$$

$$\mathbf{n}_k = [n_{br,k}^{12} \dots n_{br,k}^{1M}]^T, \quad (9c)$$

$$\mathbf{e} = [\epsilon_{br,k}^{12} \dots \epsilon_{br,k}^{1M} \eta_{br,k}^{12} \dots \eta_{br,k}^{1M}]^T. \quad (9d)$$

We assume a motion model of the moving receiver as

$$\mathbf{x}_{k+1} = \mathbf{F}_k \mathbf{x}_k + \mathbf{B}_k \mathbf{w}_{\mathbf{x}_{k,k}}, \quad (10)$$

where  $\mathbf{F}_k$  is the state-transition matrix and  $\mathbf{B}_k$  is the noise-transition matrix. Motion model (10) includes general-purpose kinematic motion models where little is known about the moving object. In the evaluation of our method in Sec. IV, we use a constant-acceleration (CA) model with the state vector

$$\mathbf{x}_k = [\mathbf{p}_{r,k} \ \mathbf{v}_{r,k} \ \mathbf{a}_{r,k}]^T, \quad (11)$$

where the components are the receiver position, velocity, and acceleration, respectively. However, note that our approach is not limited to this model. It is rather used for evaluation purposes in this paper. Using a zero-order hold sampling with sampling time  $T_s$ , the CA model is [24]

$$\mathbf{x}_{k+1} = \begin{bmatrix} \mathbf{I} & T_s \mathbf{I} & \frac{T_s^2}{2} \mathbf{I} \\ \mathbf{0} & \mathbf{I} & T_s \mathbf{I} \\ \mathbf{0} & \mathbf{0} & \mathbf{I} \end{bmatrix} \mathbf{x}_k + \begin{bmatrix} \frac{T_s^3}{6} \mathbf{I} \\ \frac{T_s^2}{2} \mathbf{I} \\ T_s \mathbf{I} \end{bmatrix} \mathbf{w}_{\mathbf{x},k}, \quad (12)$$

where  $\mathbf{w}_{\mathbf{x},k} \sim \mathcal{N}(\mathbf{0}, \mathbf{Q}_{\mathbf{x},k})$  is Gaussian distributed with covariance  $\mathbf{Q}_{\mathbf{x},k}$ . The estimation problem includes the state vector  $\mathbf{x}$ , which for our CA model is in  $\mathbf{x} \in \mathbb{R}^9$ , and the ambiguity vector  $\mathbf{n} \in \mathbb{R}^{M-1}$ . The estimation model consisting of (8) and (10) is nonlinear in the position due to the observation equations. The observations are linear in the ambiguity vector. However, a difficulty is that any dynamic evolution model of the integer ambiguities is unknown, since there can be abrupt changes in the ambiguity values from one time step to another. To reflect the uncertainty in the time evolution of the ambiguities, we describe the ambiguity with the random walk model

$$\mathbf{n}_{k+1} = \mathbf{n}_k + \mathbf{w}_{\mathbf{n},k}, \quad \mathbf{w}_{\mathbf{n},k} \sim \mathcal{N}(\mathbf{0}, \mathbf{Q}_{\mathbf{n}}), \quad (13)$$

where  $\mathbf{Q}_{\mathbf{n}}$  dominates  $\mathbf{n}_k$  in determining  $\mathbf{n}_{k+1}$  (i.e., the motion model contains little information about the ambiguity in the next time step). In a Bayesian formulation, we write (13) as

$$\mathbf{n}_{k+1} \sim p(\mathbf{n}_{k+1} | \mathbf{n}_k). \quad (14)$$

### B. Bounding the Range of Ambiguities

We leverage marginalized particle filtering for bounding the possible range of each of the ambiguities. Based on the bounded ranges, we fix the sets of integers and execute Kalman filters for each of the sets.

To bound the range of ambiguities, we start with the joint density  $p(\mathbf{x}_k, \mathbf{n}_{0:k} | \mathbf{y}_{0:k})$  of state  $\mathbf{x}_k$  and ambiguity trajectory  $\mathbf{n}_{0:k}$ , which we can decompose as

$$p(\mathbf{x}_k, \mathbf{n}_{0:k} | \mathbf{y}_{0:k}) = p(\mathbf{x}_k | \mathbf{n}_{0:k}, \mathbf{y}_{0:k}) p(\mathbf{n}_{0:k} | \mathbf{y}_{0:k}). \quad (15)$$

In resolving (15), we first estimate  $p(\mathbf{n}_{0:k} | \mathbf{y}_{0:k})$  with a particle filter using a set of  $N$  weighted particles, which results in the approximation

$$p(\mathbf{n}_{0:k} | \mathbf{y}_{0:k}) \approx \sum_{i=1}^N q_k^i \delta(\mathbf{n}_{0:k}^i - \mathbf{n}_{0:k}). \quad (16)$$

In (16),  $\delta(\cdot)$  is the Dirac delta mass and  $q_k^i$  is the associated weight for the  $i$ th particle given the measurements  $\mathbf{y}_{0:k}$ .

Given the ambiguity set  $\{\mathbf{n}_{0:k}\}_{i=1}^N$ , we execute constrained extended Kalman filters to determine  $p(\mathbf{x}_k | \mathbf{n}_{0:k}, \mathbf{y}_{0:k})$ , one for each particle. The first term on the right-hand side of (15) equals

$$p(\mathbf{x}_k | \mathbf{n}_{0:k}, \mathbf{y}_{0:k}) = \mathcal{N}(\mathbf{x}_k; \hat{\mathbf{x}}_{k|k}(\mathbf{n}_{0:k}), \mathbf{P}_{k|k}(\mathbf{n}_{0:k})), \quad (17)$$

where  $\mathcal{N}(\mathbf{x}_k; \boldsymbol{\mu}, \boldsymbol{\Upsilon})$  is the Gaussian probability density function given mean  $\boldsymbol{\mu}$  and covariance matrix  $\boldsymbol{\Upsilon}$ ,  $\hat{\mathbf{x}}_{k|k}(\mathbf{n}_{0:k})$  is the state estimate given the ambiguity trajectory  $\mathbf{n}_{0:k}$  and measurements  $\mathbf{y}_{0:k}$ , and  $\mathbf{P}_{k|k}(\mathbf{n}_{0:k})$  is its associated covariance. For brevity, we make the dependence on the ambiguity implicit in the following. The mean and covariance of the conditional

probability density function (17) using the EKF is given by the following set of equations [12],

$$\hat{\mathbf{x}}_{k|k} = \hat{\mathbf{x}}_{k|k-1} + \mathbf{K}_k(\mathbf{y}_k - \mathbf{h}_k - \lambda\bar{\mathbf{n}}_k), \quad (18a)$$

$$\mathbf{P}_{k|k} = \mathbf{P}_{k|k-1} - \mathbf{K}_k \mathbf{H}_k \mathbf{P}_{k|k-1}, \quad (18b)$$

$$\mathbf{S}_k = \mathbf{H}_k \mathbf{P}_{k|k-1} \mathbf{H}_k^T + \mathbf{R}_k, \quad (18c)$$

$$\mathbf{K}_k = \mathbf{P}_{k|k-1} \mathbf{H}_k^T \mathbf{S}_k^{-1}, \quad (18d)$$

$$\mathbf{H}_k = \left. \frac{\partial \mathbf{h}(\mathbf{x})}{\partial \mathbf{x}} \right|_{\mathbf{x}=\hat{\mathbf{x}}_{k|k-1}}, \quad (18e)$$

and the one-step prediction of the mean and covariance are given by

$$\hat{\mathbf{x}}_{k+1|k} = \mathbf{F}_k \hat{\mathbf{x}}_{k|k}, \quad (19a)$$

$$\mathbf{P}_{k+1|k} = \mathbf{F}_k \mathbf{P}_{k|k} \mathbf{F}_k^T + \mathbf{Q}_{\mathbf{x},k}. \quad (19b)$$

A key design choice in the particle filter is the proposal density  $\pi(\mathbf{n}_k | \mathbf{n}_{k-1}^i, \mathbf{y}_{0:k})$ . The standard choice is to use the prior (14), that is,  $\pi(\mathbf{n}_k | \mathbf{n}_{k-1}^i, \mathbf{y}_{0:k}) = p(\mathbf{n}_k | \mathbf{n}_{k-1})$ . However, the prediction model of the ambiguities is uninformative and the result would be that we need a huge amount of particles to ensure coverage of the true ambiguity vector. Instead, we choose the conditional distribution as proposal density,

$$\pi(\mathbf{n}_k | \mathbf{n}_{k-1}^i, \mathbf{y}_{0:k}) = p(\mathbf{n}_k | \mathbf{n}_{k-1}^i, \mathbf{y}_{0:k}). \quad (20)$$

The weight update in the particle filter is given by

$$q_k^i = \frac{p(\mathbf{y}_k | \mathbf{n}_k, \mathbf{y}_{0:k-1}) p(\mathbf{n}_k | \mathbf{n}_{k-1}^i)}{\pi(\mathbf{n}_k | \mathbf{n}_{k-1}^i, \mathbf{y}_{0:k})} q_{k-1}^i. \quad (21)$$

Inserting (20) into (21) and using the identity

$$p(\mathbf{n}_k | \mathbf{n}_{k-1}^i, \mathbf{y}_{0:k}) = \frac{p(\mathbf{y}_k | \mathbf{n}_k, \mathbf{y}_{0:k-1}) p(\mathbf{n}_k | \mathbf{n}_{k-1}^i)}{p(\mathbf{y}_k | \mathbf{n}_{k-1}^i, \mathbf{y}_{0:k-1})} \quad (22)$$

leads to the weight update

$$q_k^i \propto p(\mathbf{y}_k | \mathbf{n}_{k-1}^i, \mathbf{y}_{0:k-1}) q_{k-1}^i. \quad (23)$$

The proposal (20) is optimal in the sense that it minimizes the effect of the sampling on the weights, that is, the weights will be unaffected by  $\mathbf{n}_k^i$ , whereas other alternatives add variance to the weights [24]. It is generally difficult to sample from (20). However, the observation equation (8) is linear and Gaussian in the ambiguity vector  $\mathbf{n}$ , which is one of the few cases where exact sampling is possible [25]. For a linear and Gaussian observation equation, the optimal proposal (20) for a marginalized particle filter can be formulated as

$$p(\mathbf{n}_k | \mathbf{n}_{k-1}^i, \mathbf{y}_{0:k}) \approx \mathcal{N}(\mathbf{n}_k; \hat{\mathbf{n}}_k^i, (\Sigma_k^i)^{-1}) \quad (24a)$$

$$\hat{\mathbf{n}}_k^i = \mathbf{n}_{k-1}^i + \mathbf{K}_k^i (\mathbf{y}_k - \hat{\mathbf{y}}_{k|k-1}^i), \quad (24b)$$

$$\Sigma_k^i = ((\mathbf{S}_k^i)^{-1} + (\mathbf{Q}_n)^{-1})^{-1}, \quad (24c)$$

$$\mathbf{K}_k^i = \mathbf{Q}_n (\mathbf{Q}_n + \mathbf{S}_k)^{-1}, \quad (24d)$$

$$\hat{\mathbf{y}}_{k|k-1}^i = \mathbf{h}(\hat{\mathbf{x}}_{k|k-1}^i) + \lambda \bar{\mathbf{n}}_k^i, \quad (24e)$$

where  $\mathbf{S}_k$  is obtained from (18c). The likelihood for the weight update (23) becomes

$$\begin{aligned} p(\mathbf{y}_k | \mathbf{n}_{k-1}^i, \mathbf{y}_{0:k-1}) &= \int p(\mathbf{y}_k, \mathbf{x}_k | \mathbf{n}_{k-1}^i, \mathbf{y}_{0:k-1}) d\mathbf{x}_k \\ &= \int p(\mathbf{y}_k | \mathbf{n}_{k-1}^i, \mathbf{x}_k) p(\mathbf{x}_k | \mathbf{y}_{0:k-1}) d\mathbf{x}_k \\ &\approx \mathcal{N}(\mathbf{y}_k | \hat{\mathbf{y}}_{k|k-1}^i, \mathbf{Q}_n + \mathbf{S}_k), \end{aligned} \quad (25)$$

where  $\hat{\mathbf{y}}_{k|k-1}^i$  is obtained from (24e). Note that although the optimal proposal (24a) and therefore also the likelihood (25) are linear in the ambiguities, the covariance  $\mathbf{S}_k$  is obtained from the EKF recursion, which is approximate.

Using the proposal (24a), the generated ambiguities are real valued. However, with the particle approximation (16) of the posterior density of  $\mathbf{n}$ , using the prediction (24a) and weight update (23), we can bound the range of possible integer ambiguities as follows. After resampling with replacement, all particles have weight  $q_k^i = 1/N$  and the particle filter approximation becomes

$$p(\mathbf{n}_k | \mathbf{y}_{0:k}) \approx \hat{p}(\mathbf{n}_k | \mathbf{y}_{0:k}) = \frac{1}{N} \sum_{i=1}^N \delta(\mathbf{n}_k^i - \mathbf{n}_k). \quad (26)$$

To get a measure of the tails of the distribution for a finite number of particles, we convert the discrete representation (26) to a continuous one using a kernel density smoother [26],

$$\hat{p}_K(\mathbf{n}_k | \mathbf{y}_{0:k}) = \frac{1}{N} \sum_{i=1}^N K_h(\mathbf{n}_k^i - \mathbf{n}_k), \quad (27)$$

where  $K_h(\cdot)$  is the kernel density and  $h$  is the bandwidth. Based on the continuous density  $\hat{p}_K(\mathbf{n}_k | \mathbf{y}_{0:k})$ , we truncate (27), resulting in a continuous truncated density  $\hat{p}_{K,\text{tr}}(\mathbf{n}_k | \mathbf{y}_{0:k})$ . The truncation can, for instance, be done using the  $3\sigma$ -rule for unimodal densities, or some other suitable measure. This gives a finite set  $\mathcal{S}$  of  $N_S$  possible integer values contained in the support of  $\hat{p}_{K,\text{tr}}(\mathbf{n}_k | \mathbf{y}_{0:k})$ , that is,

$$\mathcal{S} = \{\bar{\mathbf{n}} \in \mathbb{Z}^{M-1} : \hat{p}_{K,\text{tr}}(\mathbf{n}_k | \mathbf{y}_{0:k}) > 0\}. \quad (28)$$

*Remark 1:* In this paper we make the assumption that the ambiguity prior (14) is uninformative, which means that the process noise dominates over the dynamics and that most information about the ambiguities is contained in the measurements. For the proposal (24a), it means that

$$\Sigma_k^i = ((\mathbf{S}_k^i)^{-1} + (\mathbf{Q}_n)^{-1})^{-1} \approx \mathbf{S}_k^i,$$

that is, we are effectively sampling from the likelihood.

*Remark 2:* At first sight it may seem counterintuitive to choose the ambiguities, which are linear both in the prediction model and the measurement model, to be estimated with the particle filter, especially since the observation equation is nonlinear in the receiver position. However, if the ambiguities are known, which means that the measurements are relatively highly informative about the receiver position, the nonlinearities can be handled with a Kalman-type estimator. Furthermore, using the ambiguities as particles leads to a

natural connection between marginalized particle filtering and filter banks, as will be shown in the next section.

### C. Ambiguity Resolution by Mixture Kalman Filter

Provided the  $N_S$  possible integer values in (28), we can execute a bank of  $N_S$  extended Kalman filters (or some other nonlinear estimator) to find the state vector  $\mathbf{x}_k^{\text{KF}}$ , where each filter is conditioned on the fixed integer ambiguity.

The state posterior is expressed using the law of total probability as a Gaussian mixture of  $N_S$  components,

$$\begin{aligned} p(\mathbf{x}_k^{\text{KF}} | \mathbf{y}_{0:k}) &= \sum_{i=1}^{N_S} p(\mathbf{n}^i, \mathbf{x}_k^{\text{KF}} | \mathbf{y}_{0:k}) \\ &= \sum_{i=1}^{N_S} p(\mathbf{n}^i | \mathbf{y}_{0:k}) p(\mathbf{x}_k^{\text{KF}} | \mathbf{n}^i, \mathbf{y}_{0:k}) \\ &= \sum_{i=1}^{N_S} \omega_k^i \mathcal{N}(\mathbf{x}_k^{\text{KF}} | \hat{\mathbf{x}}_{k|k}^{\text{KF},i}, \mathbf{P}_{k|k}^i), \end{aligned} \quad (29)$$

where  $\omega_k^i = p(\mathbf{n}^i | \mathbf{y}_{0:k})$  is the posterior probability of  $\mathbf{n}^i$ . The recursions for  $\hat{\mathbf{x}}_{k|k}^{\text{KF},i}, \mathbf{P}_{k|k}^{\text{KF},i}$  are in (18) with  $\bar{\mathbf{n}}$  replaced with  $\mathbf{n}^i$ . Note that  $\mathbf{n}^i$  in (29) is fixed for each Kalman filter, hence the omission of index  $k$ . The probabilities can be computed from Bayes' rule

$$\begin{aligned} \omega_k^i &= p(\mathbf{n}^i | \mathbf{y}_{0:k}) = p(\mathbf{y}_k | \mathbf{n}^i, \mathbf{y}_{0:k-1}) \frac{p(\mathbf{n}^i | \mathbf{y}_{0:k-1})}{p(\mathbf{y}_k | \mathbf{y}_{0:k-1})} \\ &\propto \omega_{k-1}^i \mathcal{N}(\mathbf{y}_k | \hat{\mathbf{y}}_{k|k-1}^i, \mathbf{S}_k^i), \end{aligned} \quad (30)$$

where the predictions  $\hat{\mathbf{y}}_{k|k-1}^i, \mathbf{S}_k^i$  are given from the corresponding Kalman filter. From (30), we choose the maximum a posteriori estimate (MAP)  $\mathbf{n}^{\text{MAP}}$  to resolve the ambiguity,

$$\mathbf{n}^{\text{MAP}} = \arg \max_{\mathbf{n}} p(\mathbf{n} | \mathbf{y}_{0:k}), \quad (31)$$

which amounts to choosing the ambiguity  $\mathbf{n}^i$  with largest  $\omega_k^i$ . The state estimate and corresponding covariance can either be obtained by the corresponding MAP or by the minimum-variance estimate [12]

$$\hat{\mathbf{x}}_{k|k}^{\text{MV}} = \sum_{i=1}^{N_S} \omega_k^i \hat{\mathbf{x}}_{k|k}^{\text{KF},i}, \quad (32a)$$

$$\mathbf{P}_{k|k}^{\text{MV}} = \sum_{i=1}^{N_S} \omega_k^i \left( \mathbf{P}_{k|k}^i + (\hat{\mathbf{x}}_{k|k}^{\text{KF},i} - \hat{\mathbf{x}}_{k|k}^{\text{MV}})(\hat{\mathbf{x}}_{k|k}^{\text{KF},i} - \hat{\mathbf{x}}_{k|k}^{\text{MV}})^T \right). \quad (32b)$$

### D. Algorithm Implementation

With the finite set of integers (28) and the mixture Kalman filter solution (29) based on this fixed, finite set, we are now ready to formulate the algorithm for joint ambiguity resolution and positioning in Algorithm 1. The method is initialized with  $N$  sets of states and ambiguities, with placeholders also for the mixture Kalman filter states (Line 1). We execute a prediction step of the ambiguities using (24a) (Line 7). If the predicted ambiguities differ from the previous ones more than some threshold  $\gamma$  (Line 9), compute the weights with

(23), from which we construct a continuous representation (27) (Line 15). From (27) we bound the range of ambiguities and fix  $N_S < N$  integer values, for which we execute Kalman filters (Line 22) to compute the MAP estimate (31) (Line 25) and state estimates (32) (Line 26). Then, we generate new samples  $\{\mathbf{n}_k^i\}_{i=1}^N$  (Lines 27–30) with indices  $\{J(i)\}_{i=1}^N$ , and restart the algorithm from Line 3.

There are a few design options in Algorithm 1. The number of particles used in the prediction when determining whether the ambiguities have changed (Lines 3–8) is a design choice that in the current implementation is fixed to  $N$ , but there are other alternatives, for instance, using  $N_S$  or some other adaptation. In determining whether the ambiguities have changed (Line 9), the distance function can be implemented in several ways. In our implementation, we simply check the largest difference in  $\{\|\mathbf{n}_k^i - \mathbf{n}_{k-1}^i\|\}_{i=1}^N$ , but more sensible choices are possible. For the choice of kernel (Line 15), there are a number of options, from which we use a Gaussian kernel. The initialization at Line 17 can, of course, be done in several ways. In the simulation study, we choose the common minimum-variance estimate over the particles for all filters. At Line 28, we draw new indices to determine the ambiguity difference in the next iteration. Here, the number of particles can be related to  $N_S$  instead of fixing it to  $N$ . Moreover, the number  $N$  used at Line 27 does not need to be fixed—it can, for instance, depend on  $N_S$ .

## IV. SIMULATION RESULTS

We present a numerical study where we have three double-differenced satellite measurements in low-earth orbit, that is, six measurements and three ambiguities. The satellites measure the distance to a moving rover with sampling time  $T_s = 0.1$  s. The rover travels on the earth-ground plane ( $p_Z = 0$ ) with nominal speed 5 m/s.

We compare with a two-stage approach based on first executing an EKF to find the float ambiguities. Then, an integer least squares is invoked, which given the float ambiguities, finds the integer ambiguities that are optimal in the least-squares sense. The integer least squares solver is the LAMBDA solver that is often used in GNSS applications, and two-stage approaches are standard for ambiguity resolution [4], [5], [21]. We denote this filter with EKF. We also compare with an idealized implementation of the EKF that knows the correct ambiguities at each time instant. Hence, this method is impossible to implement in practice, but serves as ground-truth of what can be achieved in terms of tracking performance when the ambiguities are known. The ambiguities in both filters are initialized to zero. The initial mean of the state is set to the true mean of the moving rover, and the initial covariance is

$$\mathbf{P}_0 = [100 \ 100 \ 1 \ 1 \ 1 \ 0.1]^T. \quad (33)$$

The noise parameters are the same in both filters. The code and phase measurement standard deviations are set to 0.5 m and 0.1 m, respectively.

We present results for two use-cases. The first use-case illustrates how the method performs under large initial position

**Algorithm 1** Proposed method

```

1: Initialize: Generate  $\{\mathbf{n}_{-1}^i\}_{i=1}^N \sim p_0(\mathbf{n}_0)$ ,  $\{\hat{\mathbf{x}}_{0|-1}^i\}_{i=1}^N \sim p_0(\mathbf{x}_0)$ ,  $\{\mathbf{P}_{0|-1}^i\}_{i=1}^N = \mathbf{P}_0$ ,  $\{\hat{\mathbf{x}}_{0|0}^{KF,i}\}_{i=1}^{N_S} \sim p_0(\mathbf{x}_0)$ ,  $\{\mathbf{P}_{0|0}^{KF,i}\}_{i=1}^{N_S} = \mathbf{P}_0$  and set  $\{w_i^i\}_{i=1}^N = 1/N$ .
2: for  $k = 0$  to  $T$  do
3:   for  $i = 1$  to  $N$  do
4:     Update  $\{\hat{\mathbf{x}}_{k|k-1}^i, \mathbf{P}_{k|k-1}^i\}$  using (19).
5:     Set  $\hat{\mathbf{y}}_{k|k-1}^i = \mathbf{h}(\hat{\mathbf{x}}_{k|k-1}^i) + \lambda \mathbf{n}_k^i$ .
6:     Compute  $\mathbf{S}_k^i$  from (18c).
7:     Generate  $\mathbf{n}_k^i \sim p(\mathbf{n}_k | \mathbf{n}_{k-1}^i, \mathbf{y}_{0:k})$  from (24a).
8:   end for
9:   if  $\text{dist}(\{\mathbf{n}_k^i\}_{i=1}^N, \{\mathbf{n}_{k-1}^i\}_{i=1}^N) > \gamma$  then
10:    for  $i = 1$  to  $N$  do
11:      Update  $\{\hat{\mathbf{x}}_{k|k}^i, \mathbf{P}_{k|k}^i\}$  from (18).
12:      Update  $q_k^i$  using (23) and (25).
13:    end for
14:    Resample particles to get equally weighted particles and distribution (26).
15:    Compute  $\hat{p}_K(\mathbf{n}_k | \mathbf{y}_{0:k})$  using (27).
16:    Determine  $\{\mathbf{n}_k^i\}_{i=1}^{N_S}$  using (28).
17:    Initialize  $\{\hat{\mathbf{x}}_{k|k-1}^{KF,i}\}_{i=1}^{N_S}, \{\mathbf{P}_{k|k-1}^{KF,i}\}_{i=1}^{N_S}$ .
18:  else
19:    Update  $\{\hat{\mathbf{x}}_{k|k-1}^{KF,i}, \mathbf{P}_{k|k-1}^{KF,i}\}_{i=1}^{N_S}$  using (19).
20:  end if
21:  for  $i = 1$  to  $N_S$  do
22:    Update  $\{\hat{\mathbf{x}}_{k|k}^{KF,i}, \mathbf{P}_{k|k}^{KF,i}\}$  using (18).
23:    Update weight  $\omega_k^i$  using (30).
24:  end for
25:  Compute  $\mathbf{n}^{\text{MAP}}$  using (31).
26:  Compute  $\{\hat{\mathbf{x}}_{k|k}^{\text{MV}}, \mathbf{P}_{k|k}^{\text{MV}}\}$  using (32).
27:  for  $i = 1$  to  $N$  do
28:    Draw index  $J(i)$  with probability  $\omega_k^{J(i)}$ .
29:  end for
30:  Set  $\{\mathbf{n}_k^i, \hat{\mathbf{x}}_{k|k}^i, \mathbf{P}_{k|k}^i\}_{i=1}^N = \{\mathbf{n}^l, \hat{\mathbf{x}}_{k|k}^{KF,l}, \mathbf{P}_{k|k}^{KF,l}\}_{l=J(1)}^{J(N)}$ .
31: end for

```

and ambiguity uncertainty, the transient performance, and the second use-case is cycle-slip detection. The root-mean-square-error (RMSE) at each time step and the time average of it are here used as performance measures. Let  $\mathbf{x}_{k,j}$  and  $\hat{\mathbf{x}}_{k,j}$  denote the true and estimated quantity, respectively, at time index  $k$  of the  $j$ th of  $K$  Monte-Carlo simulations. The RMSE at time step  $k$  is then computed as

$$\text{RMSE}_k = \sqrt{\frac{1}{N_{\text{MC}}} \sum_{j=1}^{N_{\text{MC}}} \|\mathbf{x}_{k,j} - \hat{\mathbf{x}}_{k,j}\|^2}. \quad (34)$$

The time-averaged RMSE is retrieved by computing the mean of the RMSE.

#### A. Transient Performance

Fig. 1 shows the position errors for the first 50 s for one of the realizations, and Fig. 2 displays the corresponding ambiguity estimation errors. The convergence of the proposed

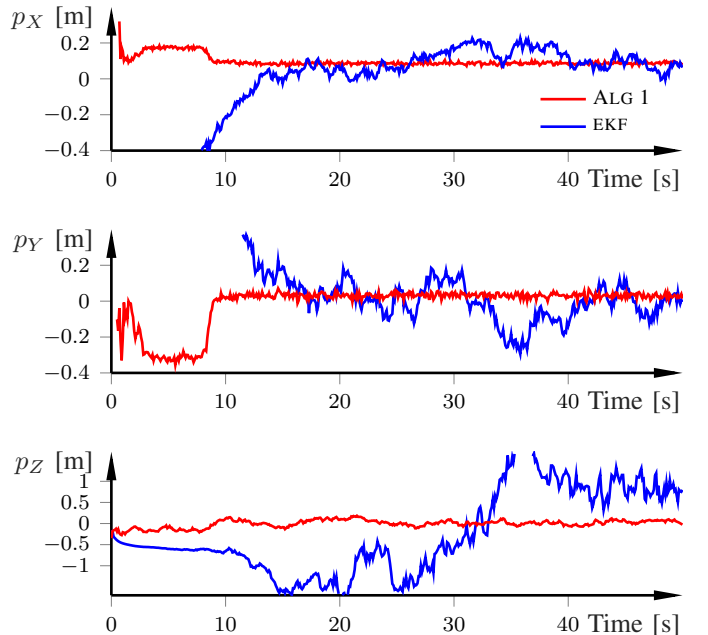


Fig. 1. Position errors for a 50 s excerpt from one realization.

method ALG 1 is considerably faster than for the two-stage approach using the LAMBDA ILS solver in combination with the EKF. Furthermore, whereas ALG 1 chooses the correct integer estimates throughout, EKF fluctuates around the correct value. In the simulations the initial position is generated from a Gaussian distribution with covariance (33). The true ambiguities are  $\{n_1, n_2, n_3\} = \{-220, 210, 175\}$  but the initial estimates are set to zero. Still, ALG 1 produces a position estimate with error less than one wavelength ( $\lambda = 0.2$  m) within a few seconds.

Fig. 3 shows the position RMSE for  $N_{\text{MC}} = 100$  Monte-Carlo executions. The convergence is faster for the proposed method compared to the two-stage approach (EKF). Furthermore, the lower bounds set by EKFIDEAL are attained within a few epochs.

Fig. 4 shows the adaptation of the number of ambiguity combinations  $N_S$  throughout the simulation. Starting from 400 particles, the number of combinations needed vary from 27 to about 500. The results indicate that the method self-adapts quickly. For periods of time,  $N_S = 3^3 = 27$  ambiguity combinations are sufficient for reliable estimation. However, when the uncertainty grows, our method can adapt to the situation and increase the number of combinations.

#### B. Cycle-Slip

Next we show the method's capabilities of detecting and compensating for cycle-slip. Fig. 5 displays the ambiguity errors and Fig. 6 shows the corresponding position errors when a cycle-slip in the satellites occur, one at a time. The proposed method (ALG 1) detects the cycle-slip almost immediately owing to the proposal used in the particle filter, and the filter tracks the correct ambiguities throughout. Moreover, the

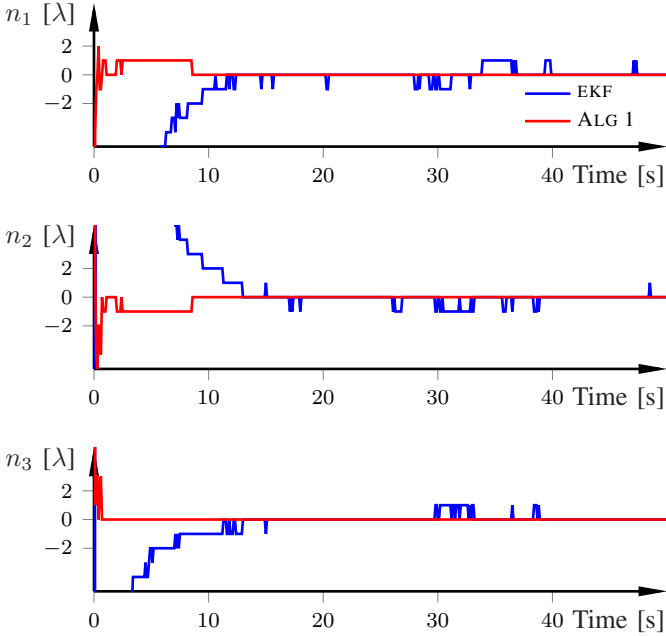


Fig. 2. Ambiguity errors corresponding to Fig. 1. The true ambiguities are  $\{n_1, n_2, n_3\} = \{-220, 210, 175\}$  and the initial ambiguity estimate is set to zero. The correct ambiguities are attained within 8 s in this realization.

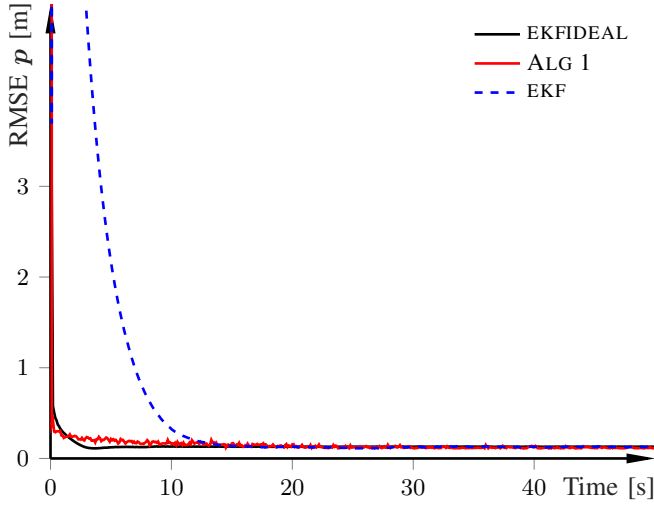


Fig. 3. Position RMSE for 100 Monte-Carlo executions. The proposed method (red) reaches steady state faster than EKF due to the fast convergence of the ambiguities, see Fig. 2.

results also indicate one of the shortcomings with a two-stage approach where both rover states and ambiguities are estimated with the EKF. When  $n_1$  changes, the two-stage approach estimates for  $n_2$  and  $n_3$  are disturbed, and similar for the other cycle-slip occasions. The reason for this unwanted behavior is the coupling in the covariance matrix amongst the different ambiguities. The cross terms yield a Kalman gain that is nonzero in the elements corresponding to the cross terms. This causes the EKF to erroneously correct  $n_2$  and  $n_3$  for changes in  $n_1$ . Clearly, from Fig. 6, the position error grows rapidly as a result of this. This behavior is not present

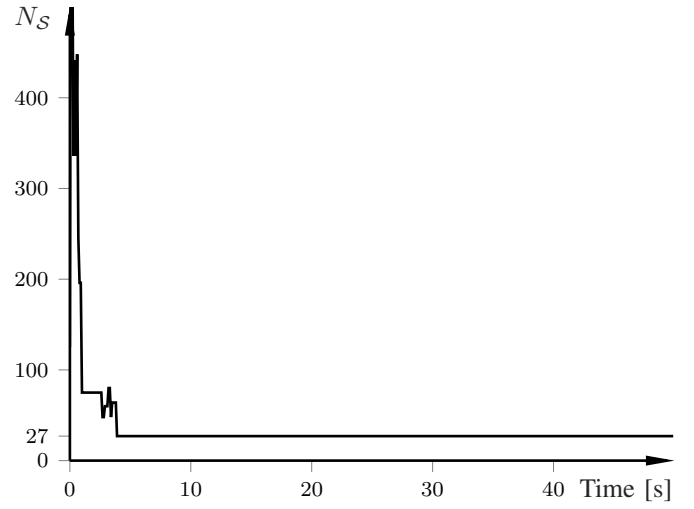


Fig. 4. The adaptation of the number of ambiguity combinations  $N_S$  from one realization.

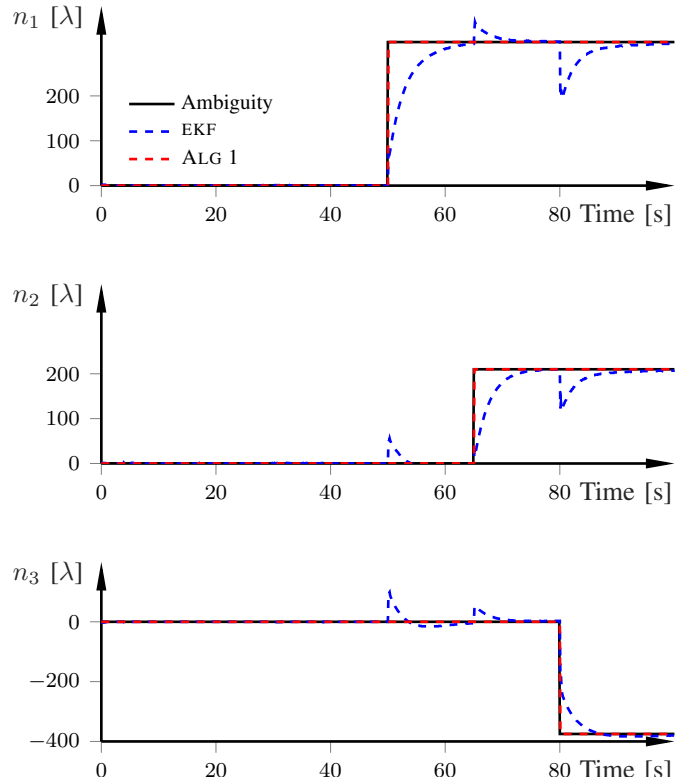


Fig. 5. Ambiguities for cycle-slip in one of the satellite trackers.

in the particle filter approach, where the marginalization and subsequent handling of the ambiguities by the particle filter decorrelates the ambiguities. Note that although it is not clear from the figure, EKF will eventually correct the positioning, but with a long transient.

## V. CONCLUSION

We addressed the GNSS positioning and ambiguity resolution problem and outlined a method based on particle filtering

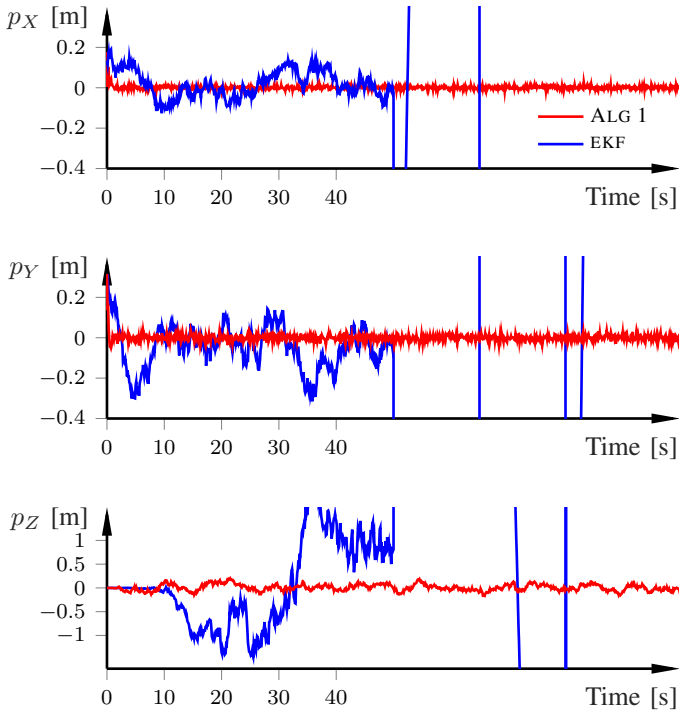


Fig. 6. Position errors for cycle-slip in one of the satellite trackers, corresponding to Fig. 5.

and mixture Kalman filters. By modeling the ambiguities as part of the nonlinear state in a marginalized approach, which at the outset is counterintuitive since the ambiguities are linear in the process and observation equations, we can use proposal sampling to guide the ambiguities to their statistically correct values. Then, we fix the ambiguities in such a way that the set of possible values contains the true ambiguities, which allows for directly finding the integer ambiguities from a mixture of Kalman filters.

The simulation study shows promising results. The method is robust to large initial uncertainties in both ambiguities and receiver position, and the estimates converge within a few seconds. Furthermore, the results indicate that the correct ambiguities are indeed contained in the determined set of integer ambiguities, meaning that should the estimate be off for one iteration, for instance, due to a poor-quality measurement, it can still recover. Cycle-slip is automatically handled in the approach and the position estimates are insensitive to the cycle-slip. Furthermore, cross-correlation between the ambiguities, which is apparent in Kalman-type methods and leads to periods of subpar estimation performance, is avoided.

In future work we will allow for loss of satellites, addition of satellites, refine the method, and include estimation of additional disturbances, such as ionospheric terms.

## REFERENCES

- [1] G. Xu and Y. Xu, *GPS: theory, algorithms and applications*. Springer, 2016.
- [2] Y. Al-Haifi, S. Corbett, and P. Cross, "Performance evaluation of GPS single-epoch on-the-fly ambiguity resolution," *Navigation*, vol. 44, no. 4, pp. 479–487, 1997.
- [3] B. Hofmann-Wellenhof, H. Lichtenegger, and J. Collins, *Global Positioning System: theory and practice*. Springer-Verlag, 1997.
- [4] P. Teunissen, "Theory of carrier phase ambiguity resolution," *Wuhan University Journal of Natural Sciences*, vol. 8, no. 2, p. 471, 2003.
- [5] S. Zhao, X. Cui, F. Guan, and M. Lu, "A Kalman filter-based short baseline RTK algorithm for single-frequency combination of GPS and BDS," *Sensors*, vol. 14, no. 8, pp. 15 415–15 433, 2014.
- [6] P. J. G. Teunissen, "A new method for fast carrier phase ambiguity estimation," in *Position Location and Navigation Symposium*, 1994.
- [7] P. J. Teunissen, "The least-squares ambiguity decorrelation adjustment: a method for fast GPS integer ambiguity estimation," *J. Geodesy*, vol. 70, no. 1, pp. 65–82, 1995.
- [8] P. D. Jonge and C. Tiberius, "The LAMBDA method for integer ambiguity estimation: implementation aspects," *Delft Geodetic Computing Centre LGR Series*, vol. 12, 1996.
- [9] X.-W. Chang, X. Yang, and T. Zhou, "MLAMBDA: a modified LAMBDA method for integer least-squares estimation," *J. Geodesy*, vol. 79, no. 9, pp. 552–565, 2005.
- [10] A. Hassibi and S. Boyd, "Integer parameter estimation in linear models with applications to GPS," *IEEE Trans. Signal Process.*, vol. 46, no. 11, pp. 2938–2952, 1998.
- [11] E. W. Grafarend, "Mixed integer-real valued adjustment (IRA) problems: GPS initial cycle ambiguity resolution by means of the LLL algorithm," *GPS Solutions*, 2000.
- [12] T. B. Schön, F. Gustafsson, and P.-J. Nordlund, "Marginalized particle filters for mixed linear nonlinear state-space models," *IEEE Trans. Signal Process.*, vol. 53, pp. 2279–2289, 2005.
- [13] B. Betti, M. Crespi, and F. Sanso, "A geometric illustration of ambiguity resolution in GPS theory and a Bayesian approach," *Manuscr. Geod.*, vol. 18, pp. 317–330, 1993.
- [14] B. Gundlich and K.-R. Koch, "Confidence regions for GPS baselines by Bayesian statistics," *J. Geodesy*, vol. 76, no. 1, pp. 55–62, 2002.
- [15] B. Gundlich and P. Teunissen, "Multiple models-fixed, switching, interacting," in *international Association of Geodesy Symposia. Volume 127. V Hotine-Marussi Symposium on Mathematical Geodesy*, 2004.
- [16] R. G. Brown and P. Y. Hwang, "A Kalman filter approach to precision GPS geodesy," *Navigation*, vol. 30, no. 4, pp. 338–349, 1983.
- [17] P. E. Henderson, J. F. Raquet, and P. S. Maybeck, "A multiple filter approach for precise kinematic DGPS positioning and carrier-phase ambiguity resolution," *Navigation*, vol. 49, no. 3, pp. 149–160, 2002.
- [18] J. D. Wolfe, W. R. Williamson, and J. L. Speyer, "Hypothesis testing for resolving integer ambiguity in GPS," *Navigation*, vol. 50, no. 1, pp. 45–56, 2003.
- [19] B. Azimi-Sadjadi and P. Krishnaprasad, "Integer ambiguity resolution in GPS using particle filtering," in *Amer. Control Conf.*, Arlington, VA, Jun. 2001.
- [20] ———, "Approximate nonlinear filtering and its application in navigation," *Automatica*, vol. 41, no. 6, pp. 945–956, 2005.
- [21] M. Sahmoudi and R. Landry, "A nonlinear filtering approach for robust multi-GNSS RTK positioning in presence of multipath and ionospheric delays," *IEEE J. Sel. Topics Signal Process.*, vol. 3, no. 5, pp. 764–776, 2009.
- [22] S. S. Hwang and J. L. Speyer, "Relative GPS carrier-phase positioning using particle filters with position samples," in *Amer. Control Conf.*, St. Louis, MO, Jun. 2009.
- [23] G. Blewitt, "Basics of the GPS technique: observation equations," *Geodetic Applications of GPS*, pp. 10–54, 1997.
- [24] F. Gustafsson, *Statistical Sensor Fusion*. Lund, Sweden: Utbildningshuset/Studentlitteratur, 2010.
- [25] M. Arulampalam, S. Maskell, N. Gordon, and T. Clapp, "A tutorial on particle filters for online nonlinear/non-Gaussian Bayesian tracking," *IEEE Trans. Signal Process.*, vol. 50, no. 2, pp. 174–188, 2002.
- [26] C. M. Bishop, *Pattern Recognition and Machine Learning*. NJ, USA: Springer-Verlag New York, 2006.